

***PtWOX11* acts as master regulator conducting the expression of key transcription factors to induce de novo shoot organogenesis in poplar**

Bobin Liu¹, Jin Zhang^{2,5}, Zhaohe Yang¹, Akihiro Matsui³, Motoaki Seki³, Shubin Li¹, Xinyang Yan¹, Markus V. Kohnen¹, Lianfeng Gu¹, Kalika Prasad⁴, Gerald A. Tuskan⁵, Mengzhu Lu², Yoshito Oka^{1,3}

¹College of Forestry, Basic Forestry and Proteomics Research Center, Fujian Agriculture and Forestry University, Fuzhou 350002, Fujian, China

²State Key Laboratory of Tree Genetics and Breeding, Research Institute of Forestry, Chinese Academy of Forestry, Beijing 100091, China

³RIKEN Center for Sustainable Resource Science, Yokohama 230-0045, Japan

⁴School of Biology, Indian Institute of Science Education and Research, Thiruvananthapuram, Kerala 695016, India

⁵Bioscience Division, Oak Ridge National Laboratory, Oak Ridge, TN 37831, USA

De novo shoot regeneration is a prerequisite for propagation and genetic engineering of elite cultivars in forestry. However, the regulatory mechanism of de novo organogenesis is poorly understood in tree species. We previously showed that *WUSCHEL (WUS)-RELATED HOMEODOMAIN 11 (PtWOX11)* of the hybrid poplar clone 84K (*Populus alba* × *P. glandulosa*) promotes de novo root formation. In this study, we found that *PtWOX11* also regulates de novo shoot regeneration in poplar. The overexpression of *PtWOX11* enhanced de novo shoot formation, whereas overexpression of *PtWOX11* fused with the transcriptional repressor domain (*PtWOX11-SRDX*) or reduced expression of *PtWOX11* inhibited this process, indicating that *PtWOX11* promotes de novo shoot organogenesis. Although *PtWOX11* promotes callus formation, overexpression of *PtWOX11* and *PtWOX11-SRDX* also produced increased and decreased numbers of de novo shoots per unit weight, respectively, implying that *PtWOX11* promotes de novo shoot organogenesis partially by regulating the intrinsic mechanism of shoot development. RNA-seq and qPCR analysis further revealed that *PtWOX11* activates the

expression of *PLETHORA1* (*PtPLT1*) and *PtPLT2*, whose *Arabidopsis* paralogs establish the acquisition of pluripotency, during incubation on callus-inducing medium. Moreover, *PtWOX11* activates the expression of shoot-promoting factors and meristem regulators such as *CUP-SHAPED COTYLEDON2* (*PtCUC2*), *PtCUC3*, *WUS* and *SHOOT MERISTEMLESS* to fulfill shoot regeneration during incubation on shoot-inducing medium. These results suggest that *PtWOX11* acts as a central regulator of the expression of key genes to cause de novo shoot formation. Our studies further provide a possible means to genetically engineer economically important tree species for their micropropagation.

Introduction

In multicellular organisms, tissue and organ regeneration is a common and widespread adaptive trait that is vital for improving survival after injury. Plants exhibit extraordinary developmental plasticity and high regeneration potential. Accordingly, plants can produce new tissues, organs and even entire plants either from individual tissues and organs or from single cells upon wounding (Sugiyama 2015; Ikeuchi et al. 2016). This high regeneration capacity has been widely used for the propagation of outstanding cultivars, genetic engineering in forestry and horticulture and in the fundamental study of plant biology (Duclercq et al. 2011; Xu and Huang 2014). De novo organogenesis can be induced under tissue culture conditions. Under such conditions, the ratio of two phytohormones, auxin and cytokinin, in the medium is the determinant of a developmental fate toward root or shoot (Skoog and Miller 1957). Although de novo organogenesis can be directly induced, it is routinely accomplished using a two-step method in

which a callus is first generated from explants during incubation on callus-inducing medium (CIM) that contains intermediate ratios of auxin/cytokinin (Duclercq et al. 2011; Xu and Huang 2014; Ikeuchi et al. 2016). The callus is then transferred to high auxin/cytokinin root-inducing medium (RIM) or low auxin/cytokinin shoot-inducing medium (SIM) to regenerate de novo roots or de novo shoots, respectively (Xu and Huang 2014).

The mechanisms underlying the formation of the callus, de novo shoots and de novo roots have been studied extensively in *Arabidopsis*. The CIM-induced callus was originally believed to be an unorganized cell mass. However, according to histological and transcriptome studies, callus has been shown to possess root-like properties resembling the lateral root primordia and a gene expression profile similar to that of root meristems (Atta et al. 2009; Sugimoto et al. 2010). Consistent with this finding, a mutation in *ABERRANT LATERAL ROOT FORMATION 4*, which promotes lateral root initiation from pericycle cells, blocks callus induction on CIM (Sugimoto et al. 2010). In addition, Kareem et al. (2015) recently demonstrated that *PLETHORA3* (*AtPLT3*), *AtPLT5* and *AtPLT7* necessary for the development of lateral root primordium (Hofhuis et al. 2013), activate the expression of *AtPLT1* and *AtPLT2*, which regulate root meristem stem cell niche establishment (Aida et al. 2004), thus establishing that the callus has the ability to form de novo shoots (Kareem et al. 2015). Thus, the genetic program that regulates lateral root formation is required not only for the formation of the callus but also for the acquisition of pluripotency by the callus (Ikeuchi et al. 2016).

De novo shoot organogenesis is a more complicated process than de novo root formation because a shoot apical meristem (SAM)-related gene set must be activated to convert a root-like cell fate into a shoot fate (Pulianmackal et al. 2014). During de novo shoot formation, the key genes required for SAM patterning are spatiotemporally regulated. The expression of *WUSCHEL*

(*AtWUS*), which maintains the identity of SAM, is expressed in the shoot progenitor region at the shoot regeneration stage (Zhang et al. 2017). *CUPSHAPED COTYLEDON1* (*AtCUC1*) and *AtCUC2*, which are required for SAM initiation and cotyledon boundary establishment (Aida et al. 1999), are up-regulated widely within the callus in plants cultured on CIM (Gordon et al. 2007). However, upon incubation on SIM, the expression of *AtCUC2* is repressed and restricted to the periphery of the *AtWUS*-expression domain (Gordon et al. 2007); under these conditions, the *AtCUC2*-expression domain proliferates, creating a developing shoot promeristem. *SHOOT MERISTEMLESS* (*AtSTM*), another regulator of SAM initiation and maintenance, is expressed in the *AtCUC2*-expression domain surrounding the shoot progenitor, where it further contributes to shoot meristem formation (Endrizzi et al. 1996; Long et al. 1996; Gordon et al. 2007). Importantly, these genes have been reported to stimulate de novo shoot organogenesis (Daimon et al. 2003; Li et al. 2011; Chatfield et al. 2013; Scofield et al. 2013). Interestingly, *AtPLT3*, *AtPLT5* and *AtPLT7* promote *AtCUC1* and *AtCUC2* expression, presumably thereby introducing the potential to form de novo shoots in the callus (Kareem et al. 2015). Thus, *AtPLT3*, *AtPLT5* and *AtPLT7* determine cell competence and stimulate shoot regeneration by regulating the expression of root stem cell regulator genes and SAM regulator genes, respectively. Recently, *WOUND-INDUCED DEDIFFERENTIATION 1* (*AtWIND1*), which plays key roles in regulating wound-induced callus formation, was reported to initiate de novo shoot organogenesis by directly and indirectly promoting the transcription of the *ENHANCER OF SHOOT REGENERATION1* (*AtESR1*) (Iwase et al. 2011, 2015, 2017). However, how the *AtPLT3/5/7*-mediated pathway and the *AtWIND1*-mediated pathway converge to regulate de novo shoot organogenesis remains unknown.

WUS-RELATED HOMEODOMAIN-CONTAINING PROTEIN 16 (*WOX*) genes encoding plant-specific homeobox family proteins fulfill key functions in plant development (Van Der Graaff et al. 2009) and have profound functions in regulating de novo organogenesis. Notably, *AtWOX11* and *AtWOX12* are involved in cell fate transition during de novo root formation in *Arabidopsis* upon wounding (Liu et al. 2014). The expression of *AtWOX11* and *AtWOX12* is induced in and surrounds the procambium cells at the wound site in an auxin-dependent manner; the expression of these genes promotes the expression of *LOB DOMAIN-CONTAINING PROTEIN 16* (*AtLBD16*) and *AtLBD29* to initiate callus and root founder cell formation (Liu et al. 2014), and later *AtWOX11/12* directly activate the expression of *AtWOX5* and *AtWOX7* for root primordium initiation (Hu and Xu 2016). It was recently reported that *AtWOX11-AtLBD16* transcriptional cascade is involved in acquisition of pluripotency in callus to promote de novo shoot organogenesis in *Arabidopsis* (Liu et al. 2018).

Poplar is an ecologically and economically important tree species that grows rapidly and produces a large amount of biomass. The determination of its genome sequence and the availability of various genetic tools has paved the way for poplar becoming a model system for studies of tree-specific traits (Jansson and Douglas 2007). Although many poplar species and genotypes are available for propagation and genetic engineering (Busov et al. 2005), many economically important species in sections *Aigerios* and *Tacamahaca* remain recalcitrant to transformation (Yevtushenko and Misra 2010). The major limitation on their availability is the failure of de novo organogenesis (Coleman and Ernst 1989). Hence, obtaining a deeper insight into the mechanisms underlying de novo organogenesis in poplar would permit future application of these species. We have previously reported that *PtWOX11* (originally referred to as *PtoWOX11/12a*), a poplar ortholog of *AtWOX11* and *AtWOX12*, promotes de novo root formation in the hybrid poplar clone 84K (*P. alba* × *P. glandulosa*) (Liu et al. 2014a, b), as is the

case in *Arabidopsis*. *PeWOX11a* and *PeWOX11b*, the *PtWOX11* orthologs from the hybrid poplar clone Nanlin895 (*P. deltoides* × *P. euramericana*) also enhance de novo root formation (Xu et al. 2015). However, little is known about the molecular mechanism of de novo shoot organogenesis in poplar.

In this study, we showed that *PtWOX11* is also involved not only in de novo root formation but also in de novo shoot formation in poplar. *PtWOX11* enhances the proliferation of the callus and the acquisition of pluripotency, presumably through the transcriptional activation of *PtPLT1* and *PtPLT2*, but not that of *AtLBD16* orthologs, during plant cultivation on CIM and SIM. In addition, upon cultivation on SIM, *PtWOX11* initiates the expression of SAM regulator genes, leading to de novo shoot organogenesis. Therefore, we propose that *WOX11* orthologs promote de novo shoot organogenesis through distinct transcriptional cascade in poplar and *Arabidopsis*.

Results

PtWOX11 promotes de novo root and de novo shoot organogenesis in poplar

We previously reported that the ectopic expression of *PtWOX11* promotes de novo root organogenesis from the stem-cutting site of the hybrid poplar clone 84K (Liu et al. 2014a, b). Here, we further tested whether *PtWOX11* promotes de novo root formation from leaf explants (Fig. 1a–c, g). In wild-type 84K, de novo roots were regenerated from 60.8% of leaf explants on RIM after 18 days after culture (DAC). The 84K leaf explants produced an average of 1.5 roots at the periphery of the cutting site (Fig. 1a, g, S1a). By contrast, 98.3% of leaf explants of the transgenic poplar overexpressing *PtWOX11* driven by the cauliflower mosaic virus 35S promoter (*PtWOX11ox*) regenerated 4.6 roots on average (Fig. 1b, g), whereas de novo root formation were severely compromised in transgenic poplar overexpressing *PtWOX11* fused with the SRDX

repression domain (Hiratsu et al. 2003) (*PtWOX11-SRDXox*) (Fig. 1c, g). Similar to 84K, *PtWOX11ox* and *PtWOX11-SRDXox* generated de novo roots from the cutting site of leaf explants (Fig. S1a–c). These data suggest that *PtWOX11* promotes de novo root formation not only from stem-cutting sites but also from leaf-cutting sites in poplar.

In 84K, de novo shoots could also be induced from 19.9% of leaf explants cultured on SIM at 18 DAC, yielding an average of 0.6 shoot on each leaf explant (Fig. 1d, h, S1d). Interestingly, *PtWOX11ox* explants exhibited an exaggerated phenotype, with up to 92.8% of leaf explants having 24 shoots on average at the leaf-cutting site (Fig. 1e, h, S1e). By contrast, only 2.9% of *PtWOX11-SRDXox* leaf explants regenerated de novo shoots (Fig. 1f, h). Similar phenotypes were observed in the other independent lines of *PtWOX11ox* and *PtWOX11-SRDXox* (Fig. S2). To confirm the function of *PtWOX11* in regulating de novo shoot formation, we established the RNAi lines for *PtWOX11* (*PtWOX11RNAi*). Expression analysis of the transgenic poplar identified 2 *PtWOX11RNAi* lines (#5 and #8) that displayed 18% (#5) and 27% (#8) reduction of *PtWOX11* transcription (Fig. S3a). In these two lines, the de novo shoot regeneration ratio was only 37.0% of that observed in 84K on SIM at 18 DAC, although the other *PtWOX11RNAi* line (#4), in which the transcriptional level of *PtWOX11* is similar to that of 84K, showed a normal phenotype of de novo shoot formation (Fig. S3b–f). Based on these results, we conclude that *PtWOX11* promotes both de novo root organogenesis and de novo shoot organogenesis in response to different auxin/cytokinin ratios. Furthermore, the function of *PtWOX11* in the regulation of de novo shoot organogenesis appeared to be organ-dependent because neither 84K, *PtWOX11ox* nor *PtWOX11-SRDXox* produced any de novo shoots from root explants, whereas *PtWOX11ox* showed enhanced de novo shoot formation from both stem explants and leaf explants (Fig. S4).

Overexpression of PtWOX11 does not alter sensitivity to phytohormones

To determine the sensitivity and responsiveness of *PtWOX11*-mediated de novo organogenesis to auxin and cytokinin in poplar, we treated 84K and *PtWOX11ox* leaf explants with various concentrations of the synthetic auxin 1-naphthaleneacetic acid (NAA) (0–6.4 μM) and the synthetic cytokinin 6-benzyladenine (BA) (0–4.44 μM) for 18 days (Fig. 2). In the 84K leaf explants exposed to high BA concentrations (2.22 and 4.44 μM), no de novo roots were formed regardless of the NAA concentration (Fig. 2a). Conversely, in 84K leaf explants exposed to low BA concentrations (0–0.88 μM), de novo roots were produced in response to NAA (Fig. 2a). In these conditions, the rate of de novo root formation in 84K leaf explants increased as the NAA concentration increased above 0.27 μM and reached 65.1% (Fig. 2f). De novo shoots were induced in 84K leaf explants by BA at all NAA concentrations tested in this study. BA concentrations of 2.22 μM and higher induced de novo shoot formation in 84K leaf explants at a rate of up to 35.0% (Fig. 2e), although BA concentrations lower than 0.88 μM hardly induced de novo shoot formation.

Interestingly, we observed a similar trend for *PtWOX11ox*; the transgenic line showed higher de novo root and shoot formation rates than 84K under all NAA/BA conditions in which de novo roots or shoots were formed in 84K (Fig. 2a, b), with the single exception when grown in 0.88 μM BA containing 6.4 μM NAA. The de novo root and shoot formation rates of *PtWOX11ox* reached 98.3% and 91.1%, respectively (Fig. 2f). These results suggest that overexpression of *PtWOX11* does not alter the sensitivity of leaf explants to auxin and cytokinin but does enhance the responsiveness of the explants to auxin and cytokinin in regulating de novo root and shoot organogenesis in an auxin/cytokinin ratio-dependent manner.

PtWOX11 promotes callus formation from the cutting site and de novo shoot regeneration

De novo shoot formation is a problematic process for many recalcitrant genotypes of poplar (Busov et al. 2005); in practical terms, it is accomplished using a two-step method. Since we observed an unexpected high shoot formation rate in *PtWOX11ox* plants, we then decided to further dissect the function of *PtWOX11* in the regulation of de novo shoot organogenesis and developed a two-step method for 84K de novo shoot regeneration. Based on the results described in the previous section (Fig. 2), we used CIM containing 3.2 μ M NAA and 0.88 μ M BA and SIM containing 3.2 μ M NAA and 2.22 μ M BA to induce de novo shoots from leaf explants and compared de novo shoot formation in 84K, *PtWOX11ox* and *PtWOX11-SRDXox* explants. On CIM, the basal side of the vein of 84K leaf explants turned red at 4 DAC, but no obvious callus formation was observed at that time (Fig. 3a). At 8 DAC, large calli had emerged along the periphery of the leaf explants, particularly at the cutting site of the vein on the basal sides of the leaf explants (Fig. 3a). To quantitatively compare callus growth, we measured the fresh weight of each callus and found that 1 g of 84K leaf explants produced 8.5 g of callus tissue (Fig. 3b). Upon transfer from CIM to SIM, de novo shoots emerged from the calli on the basal sides of the leaf explants at 16 DAC, although no morphological changes were observed at 4 or 8 DAC (Fig. 3a, S5). In the case of *PtWOX11ox* leaf explants, callus formation was visible at 4 DAC on CIM, and the calli at all cutting sites of the leaf explants were enlarged (Fig. 3a). By contrast, callus formation in *PtWOX11-SRDXox* leaf explants was compromised (Fig. 3a). Compared with 84K, a 62.5% increment and a 33.8% decrement in callus weight were observed in *PtWOX11ox* and *PtWOX11-SRDXox* leaf explants, respectively (Fig. 3b). These results indicate that *PtWOX11* promotes callus formation in leaf explants cultured on CIM.

When *PtWOX11ox* calli were transferred to SIM, a few small de novo shoots emerged from the calli at 8 DAC (Fig. 3a, S5). The de novo shoot formation rate of *PtWOX11ox* leaf explants was 70.6% at 16 DAC (Fig. 3c). By contrast, the de novo shoot formation rate was significantly reduced in case of *PtWOX11-SRDXox* leaf explants (Fig. 3c). Because *PtWOX11* promotes callus formation, the increased and decreased rates of de novo shoot formation in *PtWOX11ox* and *PtWOX11-SRDXox* leaf explants could be attributed to *PtWOX11*-mediated callus formation. However, when normalized to the fresh weight of calli *PtWOX11ox* and *PtWOX11-SRDXox* produced 2.6 times more and 0.4 times less de novo shoots as 84K (Fig. 3d), implying that *PtWOX11* promotes not only callus growth but also de novo shoot formation per se during the two-step process.

Next, we investigated whether overexpression of *PtWOX11* is sufficient for de novo shoot formation on calli. Leaf explants cultured on CIM (Fig. 4a) were transferred either to SIM (Fig. 4b) or to hormone-free medium (HFM) (Fig. 4c). *PtWOX11ox* calli produced a significantly larger number of de novo shoots on a callus weight basis than 84K on SIM (Fig. 4c, d), but the number of de novo shoots was markedly reduced on HFM (Fig. 4b, d), suggesting that an appropriate concentration of phytohormones is necessary for *PtWOX11* to promote de novo shoot formation on calli.

PtWOX11 transcription is activated during the de novo shoot formation process

The *PtWOX11* expression is restricted to the quiescent center like cells in the root apical meristem, but it is induced robustly at the cutting site during de novo root formation (Liu et al. 2014a, b). We therefore examined the expression pattern of *PtWOX11* during the process of de novo shoot formation. 84K leaf explants at various stages of de novo shoot formation induced by

the two-step method were separated into three parts (a top part that included the apical side of the leaf explant, a middle part, and a bottom part that included the basal side of the leaf explant) and subjected to reverse transcription-quantitative PCR (qPCR) analysis (Fig. 5a). As has been reported for intact plants, *PtWOX11* expression in pre-excised leaves was low (Liu et al. 2014a, b). However, robust induction of *PtWOX11* expression was observed on the basal sides of leaf explants cultured on CIM at 4 DAC, and this high expression level persisted during continued incubation on CIM. *PtWOX11* expression was also induced in the other parts of leaf explants cultured on CIM, but to a lower extent than at the base of the leaf explants (Fig. 5a).

We further examined the expression pattern of *PtWOX11* using the *pPtWOX11::GUS* line in which the expression of the β -glucuronidase (*GUS*) gene is driven by the *PtWOX11* promoter (Liu et al. 2014a, b). Consistent with the results obtained by qPCR, very little *PtWOX11* promoter activity was detected in intact leaves. In case of explants cultured on CIM, the *GUS* signal was detected along the entire periphery with the stronger promoter activity on the basal side (Fig. 5b). The expression pattern of *PtWOX11* correlated with the site of callus formation in 84K leaf explants cultured on CIM (Fig. 3a). Therefore, we concluded that *PtWOX11* is expressed at the sites at which callus formation occurs during growth on CIM. Importantly, *PtWOX11* expression was induced prior to callus appearance in 84K (Figs. 3a, 5b). In addition, strong *PtWOX11* promoter activity was still observed in calli on leaf explants cultured on CIM at 8 DAC, implying that *PtWOX11* promotes both callus initiation and callus propagation.

In contrast to the positive correlation between callus formation and *PtWOX11* expression in leaf explants cultured on CIM, the qPCR results showed that a sharp decline in *PtWOX11* transcription occurs upon transfer to SIM (Fig. 5a). Although the *PtWOX11* promoter activity in leaf explants cultured on SIM was consistently reduced, interestingly, *GUS* staining was

restricted to specific region in the swelling structures on SIM at 8 DAC (Fig. 5b, c). Further incubation on SIM drastically diminished GUS staining on the dome like structures, which are probably shoot primordium (Fig. S6), and de novo shoot (Fig. 5c).

PtWOX11 regulates the transcription of a number of genes during de novo shoot formation processes in poplar

The expression of a number of genes is regulated during de novo shoot organogenesis both in poplar (Bao et al. 2009) and in other plant species (Che et al. 2006, Su et al. 2007; Huang et al. 2014). To understand how *PtWOX11* promotes callus formation and de novo shoot formation, we analyzed genome-wide transcriptome changes in 84K and *PtWOX11ox* explants. RNA samples were collected from pre-excised leaves (leaf) and from leaf explants at 8 DAC on CIM (CIM8) and at 4 DAC (SIM4) and 8 DAC on SIM (SIM8) (Fig. 6a) as biological triplicates. We conducted a principle component analysis to examine the quality of our 24 RNA-seq samples (two genotypes × four developmental stages × three biological replicates). As shown in Fig. 6b, the principal components 1 (PC1) and PC2 explained 81.4% and 7.1% of the variance in the expression data, respectively. The three biological replicates of each genotype and developmental stage were closely clustered, indicating the high reproducibility and reliability of our RNA-seq data. PC1 separated primarily the pre-excised leaf samples from the remaining samples, while PC2 separated them according to the genotype. Interestingly, the CIM8 samples clustered further apart from both SIM samples in *PtWOX11ox* compared to 84K supporting the importance of *PtWOX11* during callus formation.

A comparison of the expression of individual genes at each time point identified numerous differentially expressed genes (DEGs) upon incubation on CIM in 84K; however, the number of

newly DEGs decreased by an order of magnitude during subsequent incubation on SIM (Fig. 6a, c, d). At CIM8 a total of 6921 and 6086 genes were up-regulated while 3152 and 3428 genes were down-regulated in 84K and *PtWOX11ox*, respectively (Fig. 6d, Table S1). By contrast, when calli were transferred to SIM, only 816 and 681 up-regulated and 386 and 527 down-regulated genes were observed at SIM4 in 84K and *PtWOX11ox*, respectively (Fig. 6d, Table S1). At SIM8 as few as 28 and 146 up-regulated and 149 and 164 down-regulated genes were identified (Fig. 6d, Table S1). In addition, the number of commonly up- or down-regulated genes at specific time points also decreased in sequential stages in both genotypes (Fig. 6e). These results are consistent with the observed trend of differential gene expression during de novo shoot formation in stems of another hybrid poplar clone, INRA 717-IB4 (*P. alba* × *P. tremula*) (Bao et al. 2009).

Although similar amounts of DEGs were identified in 84K and *PtWOX11ox* only 4895 genes and 2364 genes were commonly up- and down-regulated, respectively, in 84K and *PtWOX11ox* at CIM8 (Fig. 6f). The occurrence of commonly regulated genes decreased at SIM4 and SIM8. Accordingly, the occurrence of genes specifically regulated in 84K or *PtWOX11ox* increased as de novo shoot formation progressed (Fig. 6g, h).

Consistent with the observation that both 84K and *PtWOX11ox* form calli during culture on CIM, Gene Ontology (GO) enrichment analysis showed that genes commonly up-regulated during culture on CIM were enriched in primary metabolic processes, DNA replication, microtubule-associated processes, chitin metabolism and cellulose biosynthesis (Fig. 6i). By contrast, photosynthesis-related genes were commonly down-regulated during culture on CIM (Fig. 6i), probably because the leaf explants lost their photosynthetic properties during the process of callus formation. Interestingly, many of the GO terms that were specifically enriched

in *PtWOX11ox* for up-regulated genes at CIM8 are essential for maintaining mitochondrial function (Fig. 6i). This result may reflect the enhanced callus formation in *PtWOX11ox*, because mitochondrial energy is required for cell cycle progression (Deng et al. 2014).

In accordance with the fact that the callus undergoes the process of de novo shoot formation in response to the high cytokinin level in SIM, the GO terms for commonly up-regulated genes in SIM4 involved cell morphogenesis, developmental processes, cytokinin metabolism and two-component signaling (Fig. 6j). At SIM4, GO categories for *PtWOX11ox*-specific up-regulated genes included microtubule movement and sucrose metabolic processes (Fig. 6j), both of which might regulate the morphology and activity of SAM (Smolarkiewicz and Dhonukshe 2013; Ruan 2014; Sassi et al. 2014).

Unlike the differentially regulated genes at CIM8 and SIM4, DEGs at SIM8 overlapped poorly between 84K and *PtWOX11ox* (Fig. 6h). At SIM8, *PtWOX11ox*-specific up-regulated genes were enriched for lipid metabolic processes and fatty acid biosynthetic processes (Fig. 6k). The down-regulated genes were enriched in metabolic processes involving sugars or hormones, among others, and cell-wall-biosynthesis-related genes (Fig. 6k). These changes either are required for shoot emergence or are associated with the morphological changes that became apparent in *PtWOX11ox* at SIM8 (Fig. 3a).

PtWOX11 regulates specific transcriptional cascades during de novo shoot organogenesis

To better understand how *PtWOX11* regulates the transcriptional regulatory network during de novo shoot organogenesis, we compared the transcriptional profiles of transcription factor genes that were differentially expressed in 84K and *PtWOX11ox* at each stage (Fig. 7a–c). At CIM8, root meristem marker genes such as *PtWOX5a* and *PtWOX5b* were up-regulated in 84K and

PtWOX11ox calli (Fig. S7), suggesting that the callus has root-like properties in poplar, as is the case in *Arabidopsis* (Sugimoto et al. 2010). On the other hand, 75 and 124 transcription factors were specifically up- and down-regulated, respectively, in *PtWOX11ox* at CIM8 (Fig. 7a). Interestingly, the poplar orthologs of *AtLBD16* and *AtLBD29*, whose expression is reportedly induced by *AtWOX11* during callus formation in *Arabidopsis* (Liu et al. 2014), were not up-regulated in *PtWOX11ox* (Fig. S8). Instead, *PtLBD41* was specifically up-regulated in *PtWOX11ox* (Fig. S9a). However, *PtLBD41* is phylogenetically distinct from *AtLBD16* and *AtLBD29* (Yordanov et al. 2010). Of the 75 genes that are specifically up-regulated in *PtWOX11ox*, only *PtBBM* is thought to be involved in callus formation (Fig. S9a) since *AtBBM/PLT4* promotes callus formation in *Arabidopsis* (Boutilier et al. 2002), and *BnBBM* from *Brassica napus* promotes callus formation and shoot regeneration in tobacco (Srinivasan et al. 2007). We confirmed the up-regulation of *PtBBM* in *PtWOX11ox* on CIM by qPCR (Fig. 7d). Transcripts of *PtPLT1* and *PtPLT2*, the closest paralogs of *PtBBM*, were not detectable in our RNA-seq data. In addition, *AtPLT1* and *AtPLT2* are both involved in the acquisition of competence in *Arabidopsis* (Kareem et al. 2015). We therefore tested their expression patterns by qPCR (Fig. 7d). The number of *PtPLT1* and *PtPLT2* transcripts increased slightly at CIM8 and peaked at SIM4 in 84K. In *PtWOX11ox* transcript levels of these genes were significantly up-regulated at these time points but not in pre-excised leaves or at SIM8. Conversely, the expression of these two genes in *PtWOX11-SRDxox* was very low, indicating that *PtWOX11* activates the transcription of *PtPLT1* and *PtPLT2* in a phytohormone-dependent and/or developmental stage-dependent manner.

Upon transfer of the explants from CIM to SIM, 40 and 50 transcription factors were specifically up- and down-regulated, respectively, in *PtWOX11ox* at SIM4 (Fig. 7b). The number of

PtWOX11ox-specificly expressed genes decreased at SIM8 (Fig. 7c). However, the 20 genes that were specifically up-regulated in *PtWOX11ox* at SIM8 included genes that encode proposed key transcription factors for shoot formation and SAM maintenance, such as *PtCUC2*, *PtCUC3a*, *PtCUC3b*, *PtESR2*, *PtSPL11*, *PtSTM* and *PtWOX9* (Fig. S9b). Because *AtCUC2* and *AtESR2* have been reported to induce de novo shoot formation in *Arabidopsis*, we tested the transcription of *PtCUC2*, *PtCUC3* paralogs and *PtESR2* by qPCR analysis (Fig. 7d). These results confirmed that these genes are up-regulated in *PtWOX11ox* but down-regulated in *PtWOX11-SRDXox*, particularly at SIM8.

AtWUS and *AtSTM* are also important genes that function in cell fate determination, and they act to promote de novo shoot organogenesis in *Arabidopsis*. *PtSTM* has been reported to promote adventitious shoot formation in poplar (Groover et al. 2006). Our RNA-seq analysis revealed that *PtWUSa* and *PtSTM* were up-regulated in *PtWOX11ox* at SIM8 (Table S2), although *PtWUSa* is not included in the gene set that is specifically up-regulated in *PtWOX11ox* because of its up-regulation in 84K. Therefore, we tested the expression of these genes by qPCR. We were not able to detect the expression of *PtWUSb*, which is almost identical to *PtWUSa*, either by RNA-seq or by qPCR. In 84K, the expression of *PtWUSa* and *PtSTM* increased after incubation on SIM and reached a maximum at SIM8, although the *PtSTM* level was relatively high in pre-excised leaves (Fig. 7d). The expression of these genes was significantly higher in *PtWOX11ox* than in 84K at all stages except in the pre-incubation stage, but was repressed in *PtWOX11-SRDXox*, although the effect of *PtWOX11-SRDX* overexpression was marginal for *PtWUSa* at SIM8. Taken together, these results show that *PtWOX11* promotes the expression of potentially important genes that are orthologous to the *Arabidopsis* genes that regulate shoot formation, particularly in response to SIM.

Discussion

For decades, the regeneration of plants from differentiated plant tissue has been widely exploited in forestry and horticulture. Poplar, an ecologically and economically important plant species, is a woody plant model species that is frequently used in basic science and industrial applications. However, little is known about the molecular mechanism of de novo organogenesis in poplar. In this study, we showed that *PtWOX11* has dual functions, promoting both de novo root and shoot organogenesis in poplar as is the case in *Arabidopsis* (Fig. 1). In addition, we demonstrated that *PtWOX11* regulates de novo shoot organogenesis by regulating at least two distinct developmental events in poplar (Fig. 3). However, our RNA-seq and qPCR analysis revealed specific transcriptional cascade regulated by *PtWOX11* in poplar. Namely, *PtWOX11* activates the expression of key transcription factors such as *PtPLTs*, but not *AtLBD16* orthologs, during callus formation and that of *PtCUC2/3*, *PtWUSa* and *PtSTM* during shoot regeneration to complete the shoot formation program (Fig. 7). Therefore, our findings reveal common and different action modes of *WOX11* orthologs in regulating de novo shoot organogenesis in poplar and *Arabidopsis*.

WOX11 regulates callus formation and de novo root organogenesis in different plant species

The overexpression of *PtWOX11* and *AtWOX11* resulted in enhanced callus formation (Fig. 3a, b) (Liu et al. 2014). In *Arabidopsis*, *AtWOX11* induces the expression of *AtLBD16* and *AtLBD29* (Liu et al. 2014), which promotes callus formation (Fan et al. 2012). Consistent with the hypothesis, in which *WOX11* orthologs regulate the conserved transcriptional cascade to induce callus formation among different plant species (Hu et al. 2017), our qPCR analysis revealed that the expression of *PtLBD16a* and *PtLBD29* was significantly reduced in *PtWOX11-SRDXox* (Fig.

S8). However, unlike in *Arabidopsis*, the poplar orthologs of *AtLBD16* and *AtLBD29* were not up-regulated in leaves and calli in *PtWOX11ox* (Fig. S8) in our experimental condition. Instead, the poplar homolog of *AtBBM/PLT4*, which reportedly promotes callus formation in *Arabidopsis* (Boutilier et al. 2002), was highly expressed in *PtWOX11ox* at CIM8 (Fig. 7d). These results suggest that *PtWOX11* promotes callus formation by regulating common and partly distinct transcriptional cascades in poplar. *WOX11* orthologs promote de novo root formation in poplar, *Arabidopsis* and rice (Zhao et al. 2009; Liu et al. 2014a, b; Xu et al. 2015). However, RNA-seq and qPCR analysis revealed that the overexpression of neither *PtWOX11* nor *PtWOX11-SRDX* affect the expression of *PtWOX5a* and *PtWOX5b*, orthologs of *AtWOX5* and *AtWOX7* (Fig. S7) of which transcription is directly promoted by *AtWOX11* initiating de novo root primordia in *Arabidopsis* leaf explants (Hu and Xu 2016), in our experimental condition. In addition, expression of the orthologs of the type-A cytokinin-responsive response regulator RR2, of which expression is directly repressed by *OsWOX11* to promote adventitious root formation in rice (Zhao et al. 2009), was not repressed in *PtWOX11ox* at CIM8 (Fig. S10), while *PtRR3* and *PtRR5* expression was moderately down-regulated in explants cultured on SIM. These results imply that *WOX11* orthologs promote de novo root formation by regulating partly different transcriptional cascades during callus formation in poplar, *Arabidopsis* and rice.

PtWOX11 establishes callus competence and de novo shoot regeneration via regulating the expression of key transcription factors

Although *PtWOX11* promotes callus formation, *PtWOX11ox* produced an enormous number of de novo shoots per unit weight compared with wild-type 84K (Fig. 3a, d), suggesting that the *PtWOX11*-mediated de novo shoot organogenesis is not only the result of exaggerated callus formation but also of enhanced de novo shoot formation per se. Our phenotypic analysis also

demonstrated that the overexpression of *PtWOX11* enhances the robustness of de novo shoot formation but not its sensitivity to phytohormones (Fig. 2). Consistent with these observations, our RNA-seq analysis and qPCR analyses revealed that *PtWOX11* promotes the transcription of the orthologs of key transcription factors (Fig. 7, S9) that are essential for de novo shoot organogenesis in *Arabidopsis* (Daimon et al. 2003; Scofield et al. 2013; Zhang et al. 2017).

The acquisition of pluripotency is an important process in de novo shoot organogenesis (Che et al. 2007). Recently, *AtPLT1* and *AtPLT2* were reported to establish callus competence to induce the shoot progenitor in *Arabidopsis* (Kareem et al. 2015). Our data show that *PtWOX11* promotes *PtPLT1* and *PtPLT2* expression in calli (Fig. 7d). The induction of *PLT1* and *PLT2* during callus formation is likely a conserved mechanism (Imin et al. 2007; Kareem et al. 2015). In addition, *BnBBM* from *B. napus*, a close paralog of *BnPLT1* and *BnPLT2*, promotes not only callus formation but also adventitious shoot formation in tobacco (Srinivasan et al. 2007), arguing that the roles of *PLTs* during callus formation are conserved beyond the plant species. Furthermore, seven of the 19 GO terms enriched in *PtWOX11ox* at CIM8 overlapped with those of gene sets regulated by *AtPLT1* and *AtPLT2* (Santuari et al. 2016). Therefore, *PtWOX11* presumably promotes the acquisition of competency, at least in part, by activating the transcription of *PtPLT1* and *PtPLT2* in poplar. Interestingly, the up-regulation of *PtPLT1* and *PtBBM* in *PtWOX11ox* persists after transfer to SIM. The continuous up-regulation of these genes during culture on SIM may result in an increase in the number of de novo shoots in *PtWOX11ox* during prolonged incubation on SIM (Fig. 4d) because pluripotent calli are persistently produced even on SIM. In contrast, the expression of *AtLBD16* orthologs were not up-regulated in *PtWOX11ox* during callus formation, whereas *AtWOX11-AtLBD16* transcriptional cascade is considered to be important for establishing callus competence to

promote de novo shoot organogenesis in *Arabidopsis* (Liu et al. 2018). The lack of correlation between *PtWOX11*-induced de novo shoot formation and the expression of *AtLBD16* orthologs in poplar suggests that *WOX11* orthologs promote callus competence by regulating distinct transcriptional cascades in *Arabidopsis* and poplar. How species-dependent, *WOX11*-regulated transcriptional cascades were evolutionarily established is unknown. However, it may reflect the complexity and differences in de novo organogenesis among plant species.

The production of a pluripotent callus requires the expression of shoot-promoting factors such as *AtCUC2*, along with the expression of *AtWUS* and *AtSTM*, which act on cell fate determination to permit de novo shoot formation in *Arabidopsis*. Our RNA-seq and qPCR analysis revealed that *PtWOX11* promotes the expression of these orthologs in poplar during culture on SIM (Fig. 7d, S9). Although the function of *PtCUC2* and *PtWUS* in de novo shoot formation in poplar is still unknown, the roles of *CUC2* and *WUS* orthologs are well conserved in several plant species (Chen et al. 2009, Su et al. 2009; Larsson et al. 2012; Tanaka et al. 2015; Wang et al. 2017). In addition, the expression patterns of those genes during de novo shoot formation in poplar are similar to the patterns observed in *Arabidopsis* (Fig. 7d) (Gordon et al. 2007; Kareem et al. 2015). Therefore, it is likely that *PtCUC* s and *PtWUS*a play important roles in regulating de novo shoot organogenesis in poplar. Furthermore, *PtSTM* promotes the regeneration of adventitious shoots from leaves and roots in poplar (Groover et al. 2006). Taken together, the data suggest that *PtWOX11* works as a master regulator that coordinates the expression of *PtPLT1*, *PtPLT2*, *PtCUC* s, *PtWUS*a and *PtSTM*, which together promote the acquisition of pluripotency and shoot formation. Alternatively, *PtWOX11*-induced de novo shoot organogenesis and *PtCUC* s, *PtWUS*a and *PtSTM* expression are possibly the result of *PtWOX11*-mediated acquisition of pluripotency in poplar as is the case in *Arabidopsis*.

However, the acquisition of pluripotency and shoot formation are likely uncoupled. In addition, spatiotemporal aspects of transcription may define the differing roles of *WOX11* orthologs in regulating shoot regeneration from callus in poplar and *Arabidopsis*: unlike the expression of *AtWOX11*, which is limited to the sites of callus initiation in *Arabidopsis* (Liu, Sheng *et al.* 2014, Liu *et al.* 2018), the *PtWOX11* expression domain includes not only sites of callus initiation and propagation but also shoot primordium like structure in poplar (Fig. 5c, S6).

AtPLT3, *AtPLT5* and *AtPLT7* promote the expression of *AtPLT1*, *AtPLT2*, *AtCUC2* and *AtWUS*, thereby inducing de novo shoot formation in *Arabidopsis*. The fact that overexpression of *PtWOX11* does not activate the expression of *PtPLT5a*, *PtPLT5b* and *PtPLT3/7* in poplar (Fig. S11) indicates that *PtWOX11* does not act upstream of *PtPLT3/5/7* in the transcriptional cascade. However, whether *PtWOX11* acts as the counterpart of *AtPLT3/5/7*, whether it acts downstream of *PtPLT3/5/7* or whether they act together to promote de novo shoot organogenesis in poplar is currently unknown. These questions need to be addressed in the future to fully understand the transcriptional cascade that promotes de novo shoot organogenesis in poplar.

How *PtWOX11* regulates the expression of *PtCUC* s, *PtWUS* and *PtSTM* during de novo shoot organogenesis in poplar is currently unknown. The fact that *PtWOX11ox* largely depend on external phytohormones to initiate de novo shoot formation even after the acquisition of pluripotency (Fig. 4) suggests that phytohormone signals may modify the activity of *PtWOX11* or hormone regulated gene expression in turn is necessary for *PtWOX11*, resulting in promotion of the expression of *PtCUC* s, *PtWUS* and *PtSTM*. However, overexpression of *PtWOX11* did not affect the phytohormone sensitivity of de novo shoot organogenesis, suggesting that the phytohormone signal independently regulates de novo shoot organogenesis. Recent work has shown that the cytokinin-mediated induction of *AtWUS* during shoot regeneration is achieved

through the removal of epigenetic modifications by cytokinin in *Arabidopsis* (Zhang et al. 2017). In addition, the putative WOX11-binding motifs are localized in the promoter regions of these genes in poplar (Table S3). Indeed, PtWOX11 interacts with putative WOX11-binding cis element, TTA ATG G (Zhao et al. 2009), and activates reporter gene expression in yeast and tobacco leaves (Fig.S12), suggesting that PtWOX11 directly regulates the expression of these genes during de novo shoot regeneration processes. Therefore, it is of great interest to test how epigenetic modification of their promoters affects the PtWOX11-mediated regulation of their expression.

PtWOX11 requires a wound signal to initiate de novo organogenesis

The callus induced at a wound site is a source of subsequent tissue regeneration (Iwase et al. 2015). In *Arabidopsis*, *AtWOX11* and *AtWIND1* are key regulators that play central roles in the cellular reprogramming in response to the wound (Iwase et al. 2011; Liu et al. 2014). *AtWOX11* and *AtWIND1* are transcriptionally induced at wound sites and promote regeneration to de novo shoots. Similarly, in poplar, *PtWOX11* expression is induced in response to wounding (Fig. S13), and *PtWOX11* promotes callus formation and both root and shoot formation (Figs. 1, 3).

Although *PtWOX11* expression is wound-inducible (Fig. S13), the overexpression of *PtWOX11* still requires a wound signal to initiate callus and de novo shoot formation. This effect is shown by the fact that calli and shoots were formed only locally in the periphery of *PtWOX11ox* leaf explants (Fig. 3, S1). This result is strikingly different from the overexpression of *AtWIND1*, which induces callus and shoot formation in the absence of a wound signal (Iwase et al. 2011, 2015). *AtWIND1* promotes the expression of *AtESR1* by directly binding to its promoter and thereby indirectly regulates the cytokinin-sensitive pathway and that of *AtESR2* through the up-

regulation of *AtESR1* to promote de novo shoot regeneration (Iwase et al. 2017). It is important to note that *PtWOX11* differs from *AtWIND1* in its involvement in the regulation of cytokinin sensitivity. Whereas overexpression of *PtWOX11* does not alter cytokinin sensitivity (Fig. 2), overexpression of *AtWIND1* does (Iwase et al. 2011). In addition, our RNA-seq analysis showed that overexpression of *PtWOX11* does not promote the expression of *PtWIND1s* (Fig. S14). Therefore, it is tempting to speculate that *PtWOX11* and *PtWIND1s* act in independent transcriptional cascades to regulate de novo shoot formation. It should be noted here that the overexpression of *PtWOX11-SRDX* has little effect on SIM-induced elevation of *PtWUSa* expression and the *PtWOX11-SRDX*-mediated inhibition of shoot regeneration is leaky albeit weakly in the two-step method (Fig. 3). However, the overexpression of *PtWOX11-SRDX* almost completely blocks CIM-induced expression of *PtBBM* and *PtPLT1/2* (Fig. 7d). This suggests that a pathway other than the *PtWOX11*-*BBM/PLT1/PLT2* pathway is involved in de novo shoot regeneration in poplar. For example, *PtWIND1s* may regulate such *PtWOX11*-independent pathway. Interestingly, both *PtWOX11* and *AtWIND1* regulate the expression of *ESR2* orthologs, implying that the *PtWIND1s*-mediated wound signal and the *PtWOX11*-mediated transcriptional cascade converge at or upstream of *PtESR2* expression. However, because poplar lacks an *AtESR1* ortholog (Vahala et al. 2013), whether and how *PtWIND1s* contribute to the regulation of de novo shoot organogenesis in poplar remains unclear. Nevertheless, *PtWIND1s* are strong candidates for agents that convey the wound signal to the mechanisms that regulate *PtWOX11*-mediated de novo shoot formation because of their conserved sequence, their functions beyond plant species (Iwase et al. 2013), and their wound-responsive expression patterns in poplar (Fig. S13).

It is also possible that *PtWIND1s* regulate the expression of *PtWOX11* during de novo shoot regeneration, although they would also need to regulate both the wound-independent, cytokinin-sensitive transcriptional cascade and the *PtWOX11*-mediated transcriptional cascade in this case. These possibilities regarding the function of *PtWIND1s* should be tested in future studies to examine the possible link between the wound signal and *PtWOX11*-mediated shoot organogenesis in poplar.

The current findings define the function of *PtWOX11* and provide new insights into de novo organogenesis in poplar. *PtWOX11* is a multifunctional transcription factor that promotes three mechanistically distinct processes (callus formation, de novo root formation and de novo shoot formation) in a context-dependent manner. In addition, poplar has a specific mechanism, in which *PtWOX11* regulates the transcription of potential key transcription factors to induce de novo shoot organogenesis (Fig. 8). The molecular mechanism of de novo organogenesis in poplar is just beginning to be understood. Further investigations of the mechanism underlying both *PtWOX11*-mediated transcription and the functions of other key transcription factors will undoubtedly improve our understanding of de novo organogenesis in poplar and facilitate the availability of difficult poplar genotypes for academic study and industrial use.

Materials and methods

Plant materials and growth conditions

The hybrid poplar clone 84K (*P. alba* × *P. glandulosa*) was used in this study. *PtWOX11ox* and *pPtWOX11::GUS* have previously been described (Liu et al. 2014a, b). For propagation, plants were grown on 1/2 Murashige and Skoog (MS) medium supplemented with 0.011 μM NAA,

0.011 μM indole-3-butyric acid, 0.8% (w/v) agar and 0.088 mol/L sucrose at pH 5.8 (vegetative medium) at 23 ± 2 °C under a 16-h light ($40 \mu\text{mol m}^{-2} \text{s}^{-1}$)/8-h dark photoperiod.

Callus formation and regeneration assay in poplar

Direct shoot induction was performed according to Liu et al. (2014a, b), with modifications. Seedlings of 84K, *PtWOX11ox* and *PtWOX11-SRDXox* were grown on vegetative medium for 40 days, and the 3rd – 5th leaves were cut into approximately 0.4×0.4 -mm leaf explants under sterile conditions. The leaf explants were cultured directly on SIM (MS basal medium supplemented with 2.22 μM BA, 0.27 μM NAA, 0.8% (w/v) agar, and 0.088 M sucrose at pH 5.8). The number of de novo shoots was counted at 18 DAC. De novo shoots of poplar were distinguished as described for *Arabidopsis* (Daimon et al. 2003). For direct root induction, leaf explants were cultured directly on RIM (MS basal medium supplemented with 3.2 μM NAA, 0.8% agar, and 0.088 M sucrose at pH 5.8), and the number of de novo roots was counted at 18 DAC. For the two-step method, leaf explants were grown on CIM (MS basal medium supplemented with 0.88 μM BA, 3.2 μM NAA, 0.8% agar, and 0.088 M sucrose at pH 5.8) for 8 days and then transferred onto SIM (MS basal medium supplemented with 2.22 μM BA, 3.2 μM NAA, 0.8% agar, and 0.088 M sucrose at pH 5.8). It should be noted that the SIM used in the two-step method differs from the SIM used for direct shoot induction. To test for phytohormone sensitivity, leaf explants from 84K and *PtWOX11ox* were cultured directly on MS basal medium supplemented with various concentrations of BA and NAA, 0.8% agar, and 0.088 M sucrose at pH 5.8. The de novo shoot or root regeneration ratio was determined at 18 DAC. To estimate the fresh weight of the callus, the initial fresh weight of the explant was subtracted from that of the explant cultured on CIM.

RNA extraction, RNA sequencing and qPCR analysis

For RNA-seq, samples from different developmental stages (leaf, CIM8, SIM4 and SIM8) of 84K and *PtWOX11ox* poplar strains during de novo shoot organogenesis were collected. For each sample, 5 explants were pooled, and three biological replicates were used in this study. Total RNA was extracted using an RNAprep Pure plant kit (Tiangen, Beijing, China). The total RNA was treated with RNase-free DNase I (Tiangen, Beijing, China) to remove contaminating genomic DNA. RNA libraries were constructed using the deoxyuridine triphosphate method (Parkhomchuk et al. 2009) and sequenced with Illumina HiSeq 2500 V4. After filtering out low-quality reads, RNA-seq reads were aligned to the *P. trichocarpa* genome (version 3.0, https://phytozome.jgi.doe.gov/pz/portal.html#!info?alias=Org_Ptrichocarpa) using TopHat (version 2.0.13) (Kim et al. 2013). 70.0% of the reads were successfully mapped to the poplar genome. Differentially expressed genes (DEGs) were identified using the R package edgeR (Robinson et al. 2010). Raw *P*-values were adjusted for multiple comparison effects using the *q*-value (false discovery rate) method (Storey and Tibshirani 2003). The cut-off criteria for significantly DEGs were an absolute fold change (FC) > 2 and a *q*-value < 0.05. Principal component analysis was conducted based on the genome-wide gene expression data from all the samples using R software (Jolliffe 1986). GO enrichment analysis was performed in R using topGO (version 2.26.0) (Alexa et al. 2006).

For qPCR analysis, RNA was extracted using an RNAprep Pure plant kit (Tiangen, Beijing, China), and the contaminating genomic DNA was removed using RNase-free DNase I (Tiangen, Beijing, China). A PrimeScript™ RT reagent kit with gDNA Eraser (TaKaRa Biotechnology (Dalian), Dalian, China) was used for first-strand cDNA synthesis. qPCR primers were designed using Primer3 software (<http://frodo.wi.mit.edu/primer3/input.htm>). Real-time qPCR was

conducted using gene-specific qPCR primers (Table S1) and GoTaq® qPCR Master Mix kit (Promega, Madison, WI, USA) on a QuantStudio™ 6 qPCR system (Applied Biosystems by Life Technologies) with three independently biological repeats according to the manufacturer's instructions. The qPCR signals were normalized to that of the reference gene *PtTUB* using the Δ CT method.

GUS assay

For the GUS staining, samples of *pPtWOX11::GUS* were harvested at the pre-culture stage (leaf) or at the indicated time points during cultivation using the two-step method. GUS assay were carried out as reported method (Liu et al. 2014a, b).

Vectors and transformation

To construct the *PtWOX11-SRDXox* binary vector, the Gateway cloning system (Life Technologies, Carlsbad, CA, USA) was used. The *PtWOX11* coding sequence was amplified by PCR using a forward primer containing attB1 and a reverse primer containing the sequence encoding both the SRDX peptide (Hiratsu et al. 2003) and the attB2 sequence (Table S4). The PCR product was cloned into pDONR222 and then subcloned into pMDC32 to produce the *PtWOX11-SRDXox* vector. The binary vector was transformed into poplar using the agrobacterium-mediated method (Liu et al. 2014a, b).

DNA binding and transactivation assay

To analyze PtWOX11 transcriptional activity in yeast, the full-length *PtWOX11* and *AtWOX11* were cloned into pGBKT7 vector (Takara Bio USA, Inc. CA, USA). pGBKT7 vector harboring Gal4 binding domain fused to *PtWOX11* (BD-PtWOX11) and *AtWOX11* (BD-AtWOX11) and

empty pGBKT7 vector were transformed into the yeast strain Y2HGold containing *His3* reporter gene under the control of Gal4-responsive promoter according to Yeast Protocol Handbook (Takara Bio USA Inc., CA, USA). Transformed yeast cells were cultured on the SD plates with or without 130 μ M His for 2 days to observe transcriptional activity in yeast.

For the Yeast-One-Hybrid assay, 3 repeats of the putative WOX11-binding sequence (TTA ATG G) was cloned into pAbAi vector (Takara Bio USA, Inc. CA, USA) by Seamless Cloning system (Transgen Biotech, Beijing, China) to create 3 \times TTA ATG G-pAbAi vector. 3 \times TTA ATG G-pAbAi was transformed into yeast strain Y1HGold after linearized with BbsI to generate bait reporter strain according the Gold Yeast One-hybrid-Library Screening System User Manual (Takara Bio USA, Inc. CA, USA). The full length PtWOX11 and AtWOX11 fused with NLS-VP16 were cloned into *HindIII/HindIII* site of pGADT7 vector to create prey vectors. The prey vectors were transformed into the bait reporter strain. Transformed yeast cells were cultured on SD plates with or without 50 ng mL⁻¹ aureobasidin A for 2 days to observe the DNA binding capacity.

For transient assay in tobacco, 3 \times TTA ATG G was inserted into pGreenII0800 harboring the luciferase (*LUC*) gene (Hellens et al. 2005) to generate 3 \times TTA ATG G::*LUC* reporter construct using Seamless Cloning system (Transgen Biotech, Beijing, China). Full length *YFP* and *PtWOX11* were cloned into pMDC32 vector to produce 35S::*YFP* and 35S::*PtWOX11* effector constructs, respectively. The effector and reporter constructs were transformed into *Agrobacterium tumefaciens* strain GV3101. The *Agrobacterium* strain harboring effector construct (35S::*YFP* or 35S::*PtWOX11*) and reporter construct (3 \times TTA ATG G::*LUC*) were cocultured and the suspension was introduced into tobacco leaves lower epidermis as previously described (Liu et al. 2014a, b). The transfected leaf was sprayed with 100 μ M luciferin

(Promega, Madison, WI, USA) 48 h after transformation and kept in the dark for 5 min. The bioluminescence was observed and photographed using a cold CCD camera (Tanon-5200, Tanon, Shanghai, China). The relative luciferase activity was quantified with ImageJ.

Acknowledgements

We thank Dr. Lin Xu (Chinese Academy of Sciences, Shanghai) and Momoko Ikeuchi (RIKEN Center for Sustainable Resource Science) for critical comments on this study. This work was supported by the National Natural Science Foundation of China (Grants 31500548 to BL and 31650110478 to YO), Developmental Program for Distinguished Young Scholars of Fujian Province (2017 to BL), Natural Science Foundation of Fujian province, China (Grant 2017J01605 to YO) and by the National Key R&D Program of China (Grants 2016YFD0600106 to LG). The authors declare no conflict of interest.

References

- Aida M, Ishida T, Tasaka M (1999) Shoot apical meristem and cotyledon formation during *Arabidopsis* embryogenesis: interaction among *CUP-SHAPED COTYLEDON* and *SHOOT MERISTEMLESS* genes. *Development* 126:1563–1570
- Aida M, Beis D, Heidstra R, Willemsen V, Blilou I, Galinha C, Nussaume L, Noh YS, Amasino R, Scheres B (2004) The *PLETHORA* genes mediate patterning of the *Arabidopsis* root stem cell niche. *Cell* 119:109–120
- Alexa A, Rahnenführer J, Lengauer T (2006) Improved scoring of functional groups from gene expression data by decorrelating GO graph structure. *Bioinformatics* 22:1600–1607
- Atta R, Laurens L, Boucheron-Dubuisson E, Guivarc'h A, Carnero E, Giraudat-Pautot V, Rech P, Chriqui D (2009) Pluripotency of *Arabidopsis* xylem pericycle underlies shoot regeneration from root and hypocotyl explants grown in vitro. *Plant J* 57:626–644
- Bao Y, Dharmawardhana P, Mockler TC, Strauss SH (2009) Genome scale transcriptome analysis of shoot organogenesis in *Populus*. *BMC Plant Biol* 9:132

- Boutillier K, Offringa R, Sharma VK, Kieft H, Ouellet T, Zhang L, Hattori J, Liu CM, van Lammeren AA, Miki BL et al (2002) Ectopic expression of BABY BOOM triggers a conversion from vegetative to embryonic growth. *Plant Cell* 14:1737–1749
- Busov VB, Brunner AM, Meilan R, Filichkin S, Ganio L, Gandhi S, Strauss SH (2005) Genetic transformation: a powerful tool for dissection of adaptive traits in trees. *New Phytol* 167:9–18
- Chatfield SP, Capron R, Severino A, Penttila PA, Alfred S, Nahal H, Provart NJ (2013) Incipient stem cell niche conversion in tissue culture: using a systems approach to probe early events in *WUSCHEL*-dependent conversion of lateral root primordia into shoot meristems. *Plant J* 73:798–813
- Che P, Lall S, Nettleton D, Howell SH (2006) Gene expression programs during shoot, root, and callus development in *Arabidopsis* tissue culture. *Plant Physiol* 141:620–637
- Che P, Lall S, Howell SH (2007) Developmental steps in acquiring competence for shoot development in *Arabidopsis* tissue culture. *Planta* 226:1183–1194
- Chen SK, Kurdyukov S, Kereszt A, Wang XD, Gresshoff PM, Rose RJ (2009) The association of homeobox gene expression with stem cell formation and morphogenesis in cultured *Medicago truncatula*. *Planta* 230:827–840
- Coleman GD, Ernst SG (1989) In vitro shoot regeneration of *Populus deltoides*: effect of cytokinin and genotype. *Plant Cell Rep* 8:459–462
- Daimon Y, Takabe K, Tasaka M (2003) The *CUP-SHAPED COTYLEDON* genes promote adventitious shoot formation on calli. *Plant Cell Physiol* 44:113–121
- Deng Y, Zou W, Li G, Zhao J (2014) TRANSLOCASE OF THE INNER MEMBRANE9 and 10 are essential for maintaining mitochondrial function during early embryo cell and endosperm free nucleus divisions in *Arabidopsis*. *Plant Physiol* 166:853–868
- Duclercq J, Sangwan-Norreel B, Catterou M, Sangwan RS (2011) De novo shoot organogenesis: from art to science. *Trends Plant Sci* 16:597–606
- Endrizzi K, Moussian B, Haecker A, Levin JZ, Laux T (1996) The *SHOOT MERISTEMLESS* gene is required for maintenance of undifferentiated cells in *Arabidopsis* shoot and floral meristems and acts at a different regulatory level than the meristem genes *WUSCHEL* and *ZWILLE*. *Plant J* 10:967–979
- Fan M, Xu C, Xu K, Hu Y (2012) LATERAL ORGAN BOUNDARIES DOMAIN transcription factors direct callus formation in *Arabidopsis* regeneration. *Cell Res* 22:1169–1180
- Gordon SP, Heisler MG, Reddy GV, Ohno C, Das P, Meyerowitz EM (2007) Pattern formation during *de novo* assembly of the *Arabidopsis* shoot meristem. *Development* 134:3539–3548

- Groover AT, Mansfield SD, DiFazio SP, Dupper G, Fontana JR, Millar R, Wang Y (2006) The *Populus* homeobox gene *ARBORKNOX1* reveals overlapping mechanisms regulating the shoot apical meristem and the vascular cambium. *Plant Mol Biol* 61:917–932
- Hellens RP, Allan AC, Friel EN, Bolitho K, Grafton K, Templeton MD, Karunairetnam S, Gleave AP, Laing WA (2005) Transient expression vectors for functional genomics, quantification of promoter activity and RNA silencing in plants. *Plant Methods* 1:13
- Hiratsu K, Matsui K, Koyama T, Ohme-Takagi M (2003) Dominant repression of target genes by chimeric repressors that include the EAR motif, a repression domain, in *Arabidopsis*. *Plant J* 34:733–739
- Hofhuis H, Laskowski M, Du Y, Prasad K, Grigg S, Pinon V, Scheres B (2013) Phyllotaxis and rhizotaxis in *Arabidopsis* are modified by three PLETHORA transcription factors. *Curr Biol* 23:956–962
- Hu X, Xu L (2016) Transcription factors WOX11/12 directly activate-WOX5/7 to promote root primordia initiation and organogenesis. *Plant Physiol* 172:2363–2373
- Hu B, Zhang G, Liu W, Shi J, Wang H, Qi M, Li J, Qin P, Ruan Y, Huang H et al (2017) Divergent regeneration-competent cells adopt a common mechanism for callus initiation in angiosperms. *Regeneration* 4:132–139
- Huang X, Chen J, Bao Y, Liu L, Jiang H, An X, Dai L, Wang B, Peng D (2014) Transcript profiling reveals auxin and cytokinin signaling pathways and transcription regulation during in vitro organogenesis of Ramie (*Boehmeria nivea* L. Gaud). *PLoS ONE* 9:e113768
- Ikeuchi M, Ogawa Y, Iwase A, Sugimoto K (2016) Plant regeneration: cellular origins and molecular mechanisms. *Development* 143:1442–1451
- Imin N, Nizamidin M, Wu T, Rolfe BG (2007) Factors involved in root formation in *Medicago truncatula*. *J Exp Bot* 58:439–451
- Iwase A, Mitsuda N, Koyama T, Hiratsu K, Kojima M, Arai T, Inoue Y, Seki M, Sakakibara H, Sugimoto K et al (2011) The AP2/ERF transcription factor WIND1 controls cell dedifferentiation in *Arabidopsis*. *Curr Biol* 21:508–514
- Iwase A, Mitsuda N, Ikeuchi M, Ohnuma M, Koizuka C, Kawamoto K, Imamura J, Ezura H, Sugimoto K (2013) *Arabidopsis* WIND1 induces callus formation in rapeseed, tomato, and tobacco. *Plant Signal Behav* 8:e27432
- Iwase A, Mita K, Nonaka S, Ikeuchi M, Koizuka C, Ohnuma M, Ezura H, Imamura J, Sugimoto K (2015) WIND1-based acquisition of regeneration competency in *Arabidopsis* and rapeseed. *J Plant Res* 128:389–397
- Iwase A, Harashima H, Ikeuchi M, Rymen B, Ohnuma M, Komaki S, Morohashi K, Kurata T, Nakata M, Ohme-Takagi M et al (2017) WIND1 promotes shoot regeneration through

- transcriptional activation of *ENHANCER OF SHOOT REGENERATION1* in Arabidopsis. *Plant Cell* 29:54–69
- Jansson S, Douglas CJ (2007) *Populus*: a model system for plant biology. *Annu Rev Plant Biol* 58:435–458
- Jolliffe FR (1986) Survey design and analysis. Ellis Horwood, New York Halsted Press, Chichester
- Kareem A, Durgaprasad K, Sugimoto K, Du Y, Pulianmackal AJ, Trivedi ZB, Abhayadev PV, Pinon V, Meyerowitz EM, Scheres B et al (2015) *PLETHORA* genes control regeneration by a two-step mechanism. *Curr Biol* 25:1017–1030
- Kim D, Pertea G, Trapnell C, Pimentel H, Kelley R, Salzberg SL (2013) TopHat2: Accurate alignment of transcriptomes in the presence of insertions, deletions and gene fusions. *Genome Biol* 14:R36
- Larsson E, Sundstrom JF, Sitbon F, von Arnold S (2012) Expression of *PaNAC01*, a *Picea abies* *CUP-SHAPED COTYLEDON* orthologue, is regulated by polar auxin transport and associated with differentiation of the shoot apical meristem and formation of separated cotyledons. *Ann Bot* 110:923–934
- Li W, Liu H, Cheng ZJ, Su YH, Han HN, Zhang Y, Zhang XS (2011) DNA methylation and histone modifications regulate de novo shoot regeneration in *Arabidopsis* by modulating *WUSCHEL* expression and auxin signaling. *PLoS Genet* 7:e1002243
- Liu B, Wang L, Zhang J, Li J, Zheng H, Chen J, Lu M (2014a) *WUSCHEL*-related Homeobox genes in *Populus tomentosa*: diversified expression patterns and a functional similarity in adventitious root formation. *BMC Genomics* 15:296
- Liu J, Sheng L, Xu Y, Li J, Yang Z, Huang H, Xu L (2014b) *WOX11* and *12* are involved in the first-step cell fate transition during de novo root organogenesis in *Arabidopsis*. *Plant Cell* 26:1081–1093
- Liu J, Hu X, Qin P, Prasad K, Hu Y, Xu L (2018) The *WOX11-LBD16* pathway promotes pluripotency acquisition in callus cells during de novo shoot regeneration in Arabidopsis tissue culture. *Plant Cell Physiol* 59:739–748
- Long JA, Moan EI, Medford JI, Barton MK (1996) A member of the KNOTTED class of homeodomain proteins encoded by the *STM* gene of *Arabidopsis*. *Nature* 379:66–69
- Parkhomchuk D, Borodina T, Amstislavskiy V, Banaru M, Hallen L, Krobitch S, Lehrach H, Soldatov A (2009) Transcriptome analysis by strand-specific sequencing of complementary DNA. *Nucleic Acids Res* 37:e123 Pulianmackal AJ, Kareem AV, Durgaprasad K, Trivedi ZB, Prasad K
- (2014) Competence and regulatory interactions during regeneration in plants. *Front Plant Sci* 5:142

- Robinson MD, McCarthy DJ, Smyth GK (2010) edgeR: a Bioconductor package for differential expression analysis of digital gene expression data. *Bioinformatics* 26:139–140
- Ruan YL (2014) Sucrose metabolism: gateway to diverse carbon use and sugar signaling. *Annu Rev Plant Biol* 65:33–67
- Santuari L, Sanchez-Perez GF, Luijten M, Rutjens B, Terpstra I, Berke L, Gorte M, Prasad K, Bao D, Timmermans-Hereijgers JL et al (2016) The *PLETHORA* gene regulatory network guides growth and cell differentiation in *Arabidopsis* roots. *Plant Cell* 28:2937–2951
- Sassi M, Ali O, Boudon F, Cloarec G, Abad U, Cellier C, Chen X, Gilles B, Milani P, Friml J et al (2014) An auxin-mediated shift toward growth isotropy promotes organ formation at the shoot meristem in *Arabidopsis*. *Curr Biol* 24:2335–2342
- Scofield S, Dewitte W, Nieuwland J, Murray JA (2013) The *Arabidopsis* homeobox gene *SHOOT MERISTEMLESS* has cellular and meristem-organisational roles with differential requirements for cytokinin and *CYCD3* activity. *Plant J* 75:53–66
- Skoog F, Miller CO (1957) Chemical regulation of growth and organ formation in plant tissues cultured in vitro. *Symp Soc Exp Biol* 11:118–130
- Smolarkiewicz M, Dhonukshe P (2013) Formative cell divisions: principal determinants of plant morphogenesis. *Plant Cell Physiol* 54:333–342
- Srinivasan C, Liu Z, Heidmann I, Supena ED, Fukuoka H, Joosen R, Lambalk J, Angenent G, Scorza R, Custers JB et al (2007) Heterologous expression of the *BABY BOOM AP2/ERF* transcription factor enhances the regeneration capacity of tobacco (*Nicotiana tabacum* L.). *Planta* 225:341–351
- Storey JD, Tibshirani R (2003) Statistical significance for genomewide studies. *Proc Natl Acad Sci USA* 100:9440–9445
- Su N, He K, Jiao Y, Chen C, Zhou J, Li L, Bai S, Li X, Deng XW (2007) Distinct reorganization of the genome transcription associates with organogenesis of somatic embryo, shoots, and roots in rice. *Plant Mol Biol* 63:337–349
- Su YH, Zhao XY, Liu YB, Zhang CL, O'Neill SD, Zhang XS (2009) Auxin-induced *WUS* expression is essential for embryonic stem cell renewal during somatic embryogenesis in *Arabidopsis*. *Plant J* 59:448–460
- Sugimoto K, Jiao Y, Meyerowitz EM (2010) *Arabidopsis* regeneration from multiple tissues occurs via a root development pathway. *Dev Cell* 18:463–471
- Sugiyama M (2015) Historical review of research on plant cell dedifferentiation. *J Plant Res* 128:349–359
- Tanaka W, Ohmori Y, Ushijima T, Matsusaka H, Matsushita T, Kumamaru T, Kawano S, Hirano HY (2015) Axillary meristem formation in rice requires the *WUSCHEL* Ortholog *TILLERS ABSENT1*. *Plant Cell* 27:1173–1184

- Vahala J, Felten J, Love J, Gorzsas A, Gerber L, Lamminmaki A, Kangasjarvi J, Sundberg B (2013) A genome-wide screen for ethylene-induced ethylene response factors (ERFs) in hybrid aspen stem identifies *ERF* genes that modify stem growth and wood properties. *New Phytol* 200:511–522
- Van Der Graaff E, Laux T, Rensing SA (2009) The WUS homeobox-containing (WOX) protein family. *Genome Biol* 10:248
- Wang J, Tian C, Zhang C, Shi B, Cao X, Zhang TQ, Zhao Z, Wang JW, Jiao Y (2017) Cytokinin signaling activates *WUSCHEL* expression during axillary meristem initiation. *Plant Cell* 29:1373–1387
- Xu L, Huang H (2014) Genetic and epigenetic controls of plant regeneration. *Curr Top Dev Biol* 108:1–33
- Xu M, Xie W, Huang M (2015) Two *WUSCHEL*-related HOMEBOX genes, *PeWOX11a* and *PeWOX11b*, are involved in adventitious root formation of poplar. *Physiol Plant* 155:446–456
- Yevtushenko DP, Misra S (2010) Efficient *Agrobacterium*-mediated transformation of commercial hybrid poplar *Populus nigra* L. x *P. maximowiczii* A. Henry. *Plant Cell Rep* 29:211–221
- Yordanov YS, Regan S, Busov V (2010) Members of the LATERAL ORGAN BOUNDARIES DOMAIN transcription factor family are involved in the regulation of secondary growth in *Populus*. *Plant Cell* 22:3662–3677
- Zhang TQ, Lian H, Zhou CM, Xu L, Jiao Y, Wang JW (2017) A two-step model for de novo activation of *WUSCHEL* during plant shoot regeneration. *Plant Cell* 29:1073–1087
- Zhao Y, Hu Y, Dai M, Huang L, Zhou DX (2009) The WUSCHEL-Related homeobox gene *WOX11* is required to activate shootborne crown root development in rice. *Plant Cell* 21:736–748

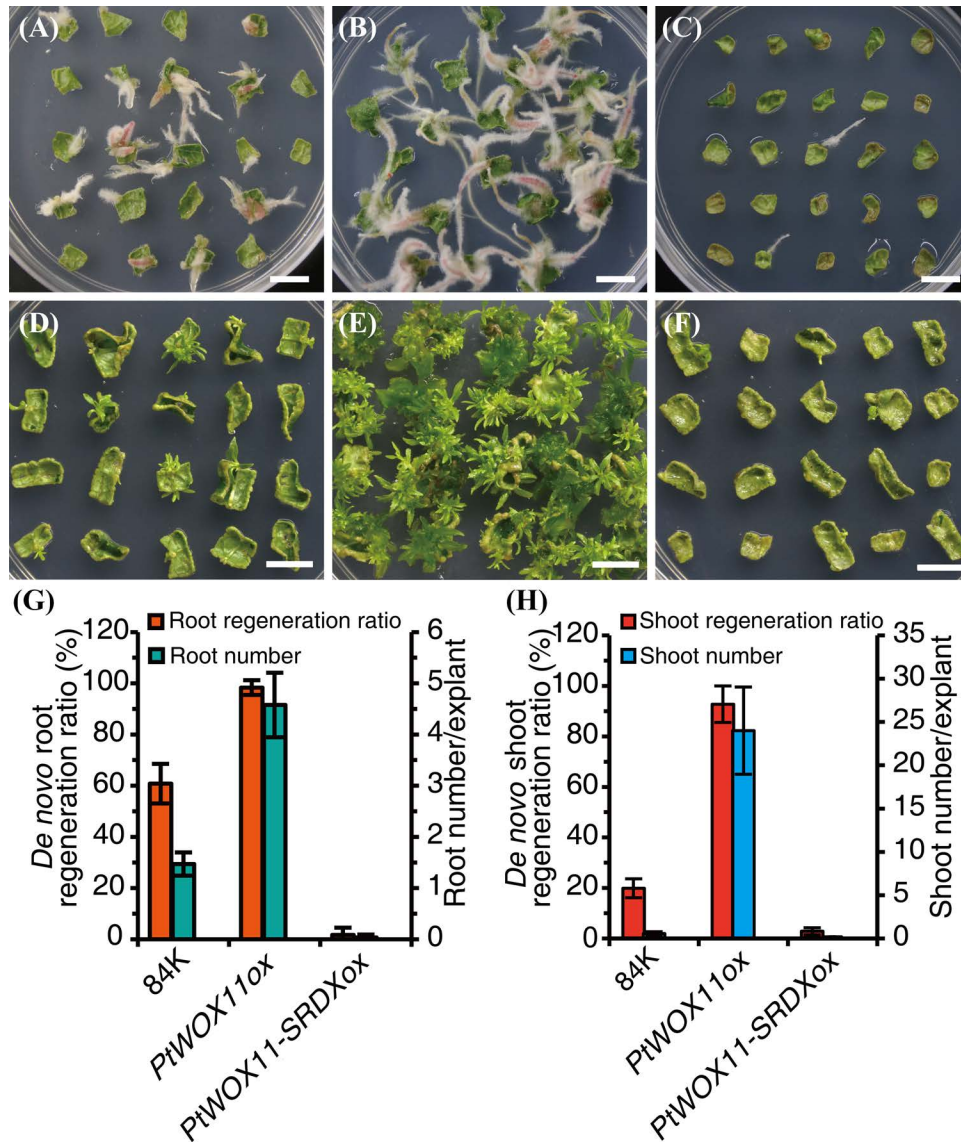


Figure 1. *PtWOX11* is involved in de novo root and shoot organogenesis from leaf explants. **a–c** Regenerated de novo roots formed by leaf explants. Leaf explants of 84K (**a**), *PtWOX11ox*#6 (**b**) and *PtWOX11-SRDXox*#19 (**c**) were cultured on RIM for 18 days. Scale bars = 1 cm. **d–f** Regenerated de novo shoots formed by leaf explants. Leaf explants of 84K (**d**), *PtWOX11ox*#6 (**e**) and *PtWOX11-SRDXox*#19 (**f**) were cultured on SIM for 18 days. Scale bars = 1 cm. **g** Quantitative analyses of de novo root organogenesis. De novo root organogenesis of the indicated genotypes was measured as the “De novo root regeneration ratio” and the “Root number per leaf explant” at 18 DAC. The bars show the SD of the values obtained for three biological repeats. n = 25 for each repeat. **h** Quantitative analyses of de novo shoot organogenesis. De novo shoot organogenesis of the indicated genotypes was measured as the “De novo shoot regeneration ratio” and the “Shoot number per leaf explant” at 18 DAC. The bars show the SD of the values obtained for three biological repeats. n = 25 in each repeat.

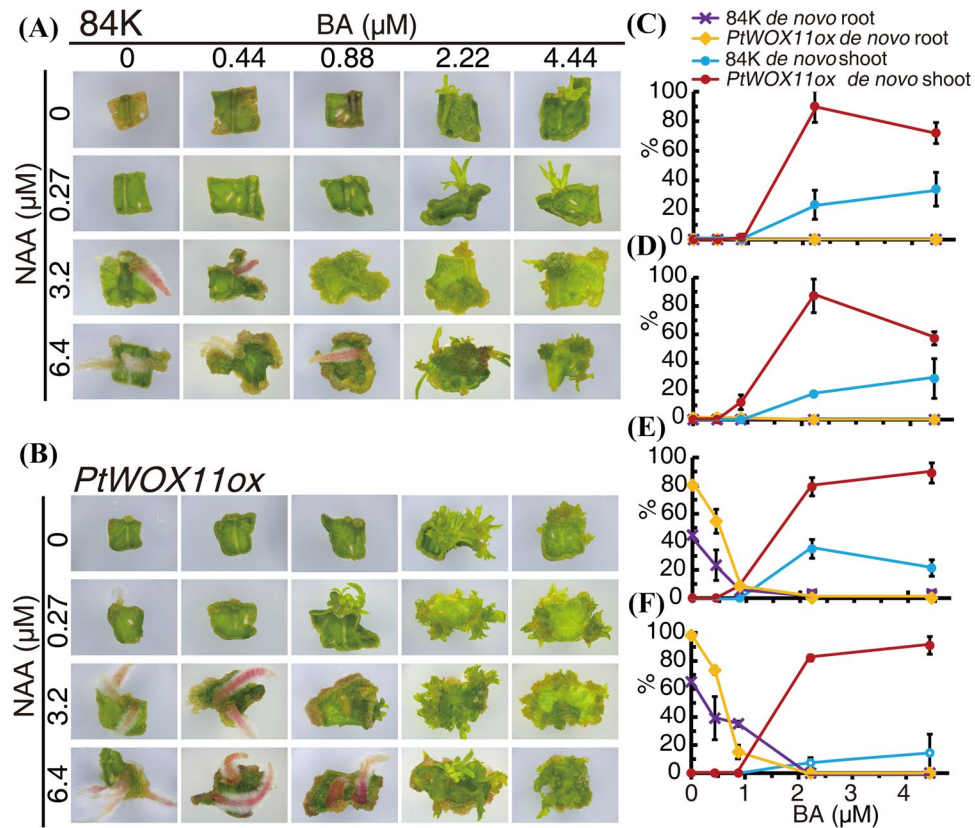


Figure 2. Responses of 84K and *PtWOX11ox* leaf explants to auxin and cytokinin. **a** and **b** Comparison of the responses of 84K (**a**) and *PtWOX11ox* (**b**) leaf explants to different auxin and cytokinin concentrations. Leaf explants were directly cultured on medium containing different concentrations of NAA and BA for 20 days. Representative images are shown. **c–f** Quantitative analyses of the *de novo* root and shoot regeneration ratio dynamics of 84K and *PtWOX11ox* leaf explants in response to different BA concentrations at NAA = 0 μM (**c**), 0.27 μM (**d**), 3.2 μM (**e**) and 6.4 μM (**f**). The bars show the SE of the values obtained for three biological repeats. $n = 25$ for each repeat.

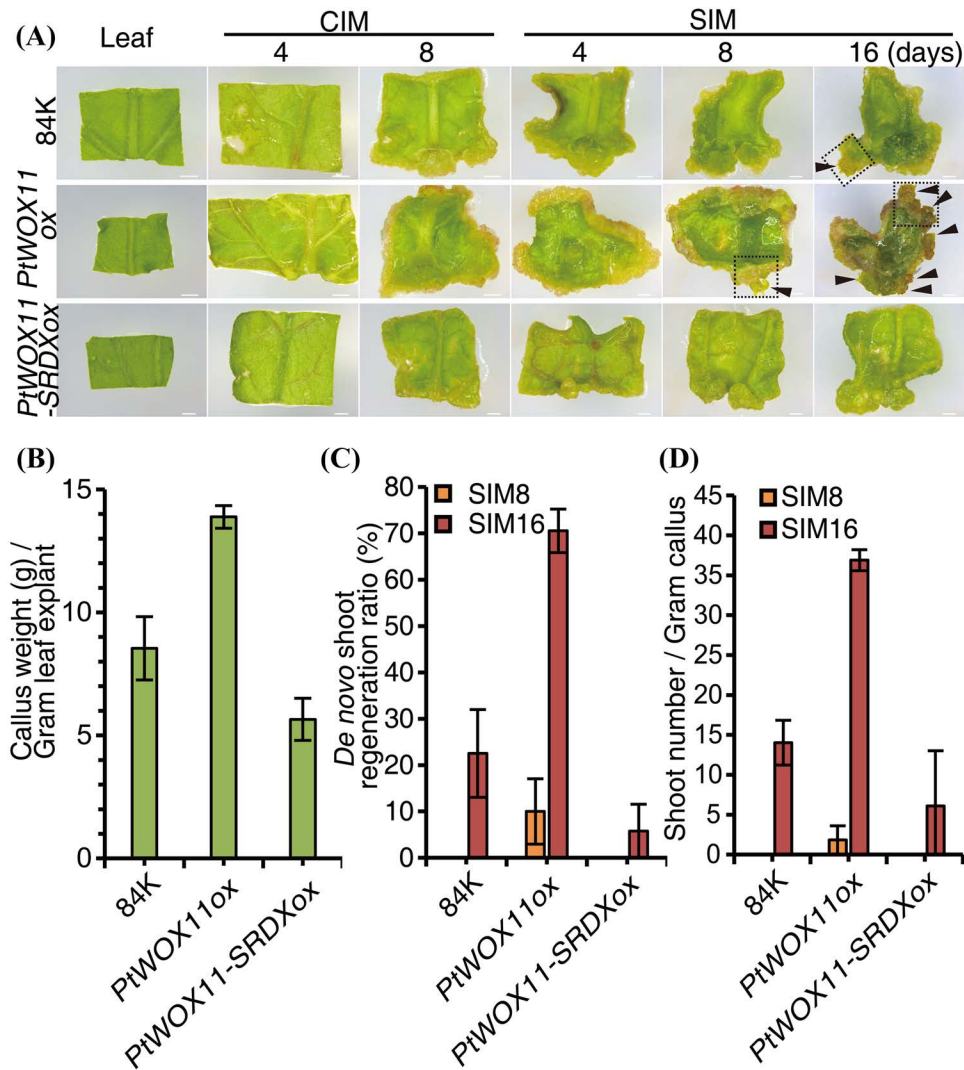


Figure 3. *PtWOX11* promotes de novo shoot formation during cultivation with the two-step method. **a** De novo shoot regeneration process during cultivation with the two-step method. Leaf explants of 84K (top), *PtWOX11^{ox}* (middle) and *PtWOX11-SRDxox* (bottom) were first grown on CIM for 8 days and subsequently cultured on SIM for 16 days. Representative images of the pre-incubated leaf explants (leaf) and the leaf explants cultured on CIM and SIM for the indicated number of days are shown. Magnified views of the de novo shoots indicated in the dotted boxes in 84K explants at 16 DAC on SIM and in *PtWOX11^{ox}* at 8 and 16 DAC on SIM are shown in Fig. S5. The leaf explants were placed with the apical side of the leaf upward. The black arrowheads indicate de novo shoots. Scale bars = 1 mm. **b** Quantification of callus formation. The weight of the callus in the indicated genotypes was measured at 8 DAC on CIM and normalized to the weight of the pre-incubated leaf explant. The bars show the SDs of the values obtained for three biological repeats. **c** and **d** Quantification of de novo shoot regeneration. De novo shoot regeneration ratio (**c**) and shoot number (**d**) of the indicated genotypes were measured at 8 and 16 DAC on SIM during cultivation by the two-step method,

as described in **a**. The shoot number is normalized to the weight of the callus measured at 8 DAC on CIM. The bars show the SD of the values obtained for three biological repeats. n = 25 for each repeat.

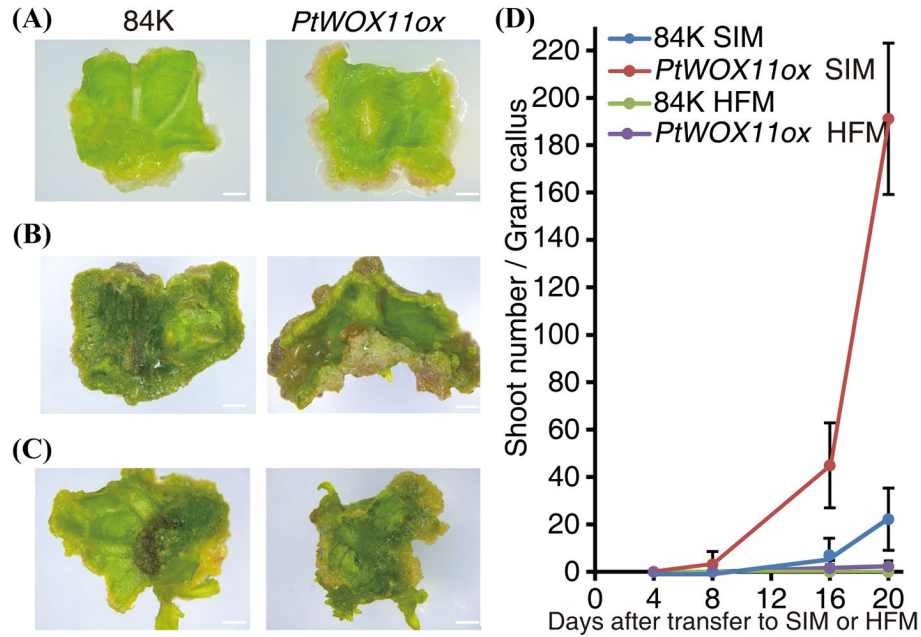


Figure 4. *PtWOX11*-mediated de novo shoot regeneration depends on phytohormones. **a** Representative images of leaf explants of 84K and *PtWOX11ox* after culturing on CIM for 8 days. The leaf explants were placed with the apical side of the leaf upward. Scale bars = 1 mm. **b** and **c** Representative images of leaf explants after transfer to hormone-free medium (HFM) (**b**) or SIM (**c**). Leaf explants of 84K and *PtWOX11ox* were grown on CIM for 8 days and subsequently cultured on HFM or SIM for 20 days. The leaf explants were placed with the apical side of the leaf upward. The black arrowheads indicate de novo shoots. Scale bars = 1 mm. **d** Quantification of the number of de novo shoots in 84K and *PtWOX11ox* leaf explants grown on HFM or SIM for the indicated numbers of days. The de novo shoot numbers were normalized to the weight of the callus at 8 DAC on CIM. The bars show the SD of the values obtained for three biological repeats. n = 25 for each repeat.

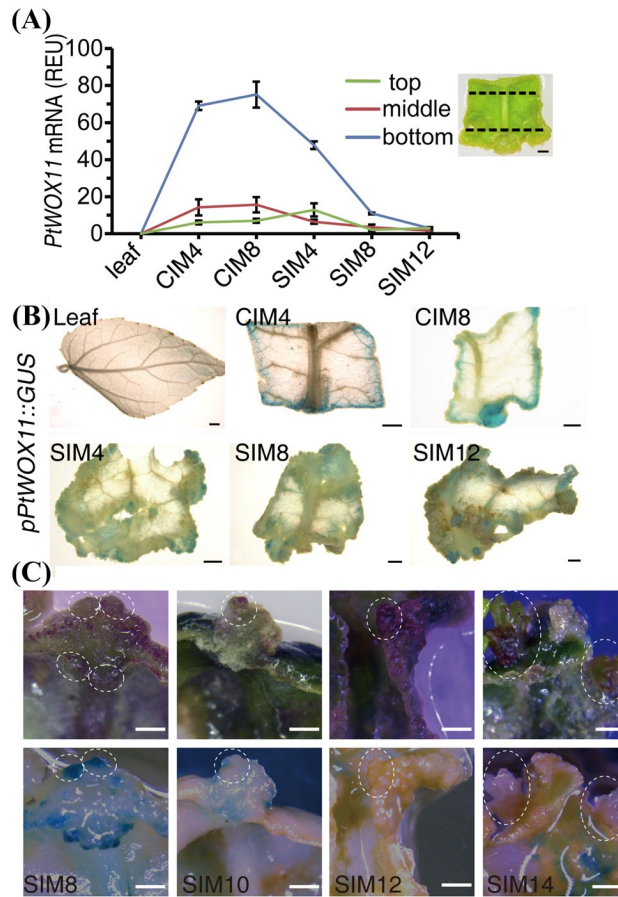


Figure 5. Expression of *PtWOX11* is activated during de novo shoot regeneration. **a** qPCR analyses of *PtWOX11* expression pattern during two-step de novo shoot regeneration processes. Leaf explants of 84K were grown on CIM for 8 days and subsequently cultured on SIM for 12 days. The samples were harvested for qPCR analysis before excision of the leaf (leaf), at 4 DAC (CIM4) and 8 DAC (CIM8) on CIM and at 4 DAC (SIM4), 8 DAC (SIM8) and 12 DAC (SIM12) on SIM. The leaf explants at each time point were separated into three parts: a top part, including the apical side of the leaf explant, a middle part, and a bottom part including the basal side of the leaf explant. Scale bar = 1 mm. The qPCR signal of *PtWOX11* expression was first normalized to the expression of *PtTUB*; the relative expression unit (REU) was then calculated by re-normalization of the normalized qPCR signal in samples to that in pre-excised leaves. **b** *PtWOX11* promoter activity during the induction of de novo shoots. Leaf explants of *pPtWOX11::GUS* were grown on CIM for 8 days and subsequently cultured on SIM for 12 days. Representative histochemical GUS staining of the pre-excised leaf and of leaf explants harvested at the indicated time points are shown. The leaf explants were placed with the apical side of the leaf upward. Scale bars = 1 mm. **c** Close-up pictures of *PtWOX11* promoter activity during the incubation on SIM. Leaf explants of *pPtWOX11::GUS* were grown on CIM for 8 days and subsequently cultured on SIM for 14 days. Representative pictures of the leaf explants harvested at the indicated time points before GUS staining (top) and after GUS staining (bottom) are

analysis. The DEGs were calculated by comparison with the prior stages for 84K (Ca, Cb and Cc) and *PtWOX11ox* (Cd, Ce and Cf). **b** Principal component analysis of 24 sets of transcriptome data from leaf, CIM8, SIM4 and SIM8 of 84K and *PtWOX11ox*. **c** Gene expression profiles in de novo shoot regeneration processes of 84K and *PtWOX11ox*. **d** The number of up- or down-regulated genes at each stage was calculated by comparison with the prior stage during twostep de novo shoot formation. **e** Venn diagrams showing the common and newly up- or down-regulated genes compared with the prior stage during de novo shoot formation processes in 84K and *PtWOX11ox*. **f–h** Venn diagrams showing the genes commonly and specifically regulated at each stage in 84K and *PtWOX11ox* during de novo shoot formation. **i–k** GO analysis of the gene sets commonly and specifically expressed in **f–h**. *UR* up-regulated, *DR* down-regulated, *NC* not changed. The gray color represents the GO terms that are not significantly overrepresented.

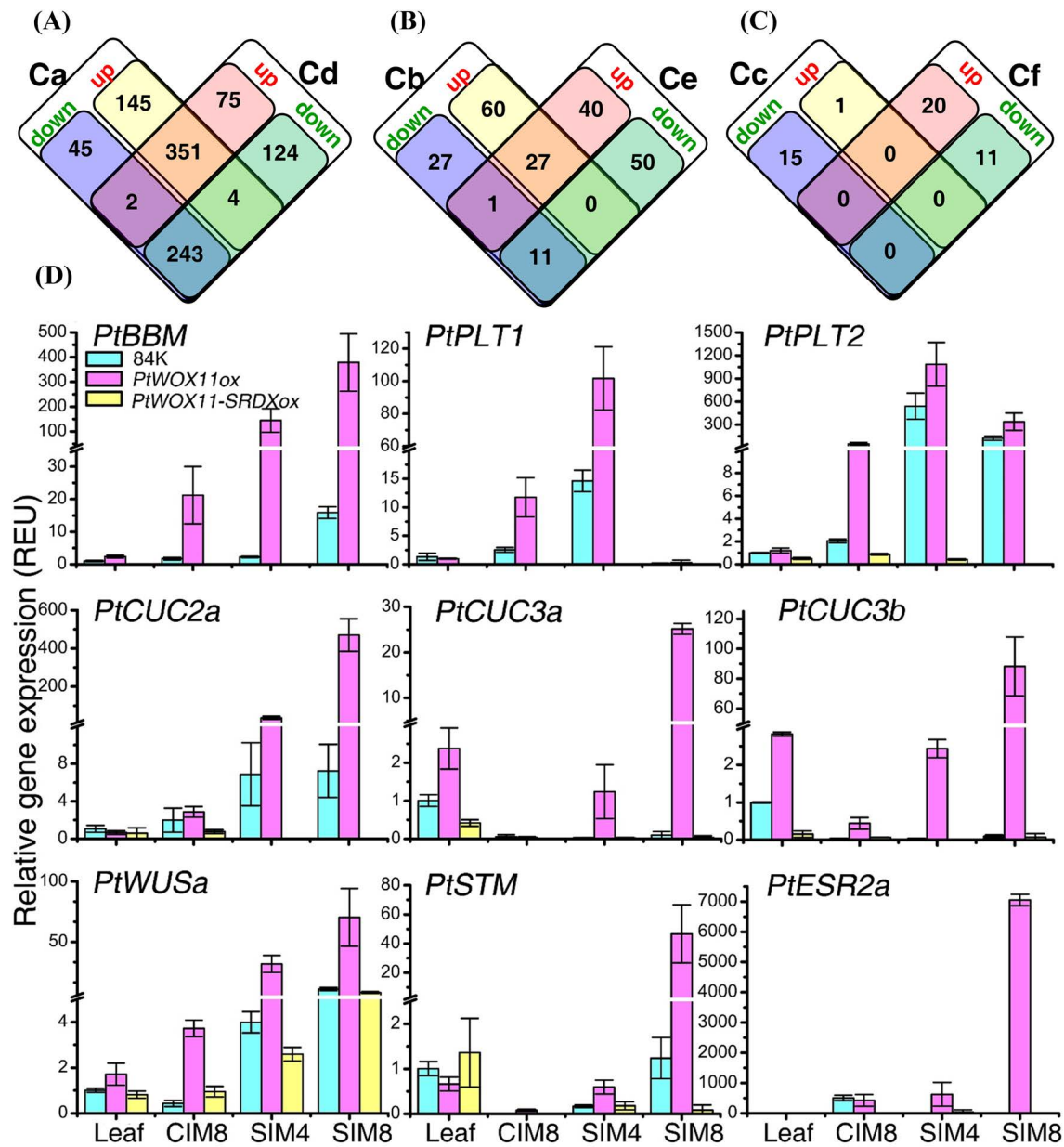


Figure 7. Transcription factor genes that are commonly or specifically regulated in 84K and/or *PtWOX1lox* during de novo shoot organogenesis. **a–c** Venn diagrams showing the transcription factor genes that are commonly and specifically regulated in 84K and/or *PtWOX1lox* at every stage during the process of de novo shoot formation. **d** qPCR analysis of the key regulators of callus formation and/or shoot regeneration. Leaf explants of 84K and *PtWOX1lox* were grown on CIM for 8 days and subsequently cultured on SIM for 8 days. RNA samples from pre-excised leaves (leaf) and from leaf explants at 8 DAC on CIM (CIM8) and at 4 DAC (SIM4) and 8 DAC on SIM (SIM8) were subjected to qPCR analysis. The qPCR signal of each gene's expression was first normalized to that of *PtTUB*; the relative expression unit (REU) was then calculated by re-normalization of the normalized qPCR signal in the sample to that in the 84K pre-excised leaf. The bars show the SD of the values obtained for three biological repeats. n = 25 for each repeat.

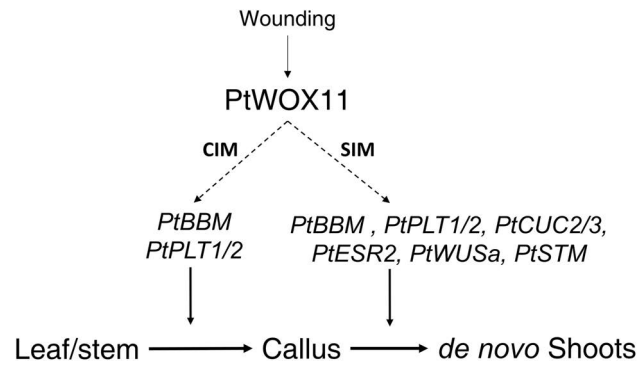


Figure 8. PtWOX11-mediated transcriptional cascade during de novo shoot regeneration in poplar. *PtWOX11* transcription can be induced by wounding. On CIM, *PtWOX11* promotes pluripotent callus formation from the cutting site by promoting the expression of *PtBBM*, *PtPLT1* and *PtPLT2*. On SIM, PtWOX11 boosts de novo shoot regeneration by up-regulating the expression of *PtBBM*, *PtPLT1*, *PtPLT2*, *PtCUC2/3*, *PtESR2*, *PtWUSa* and *PtSTM*.